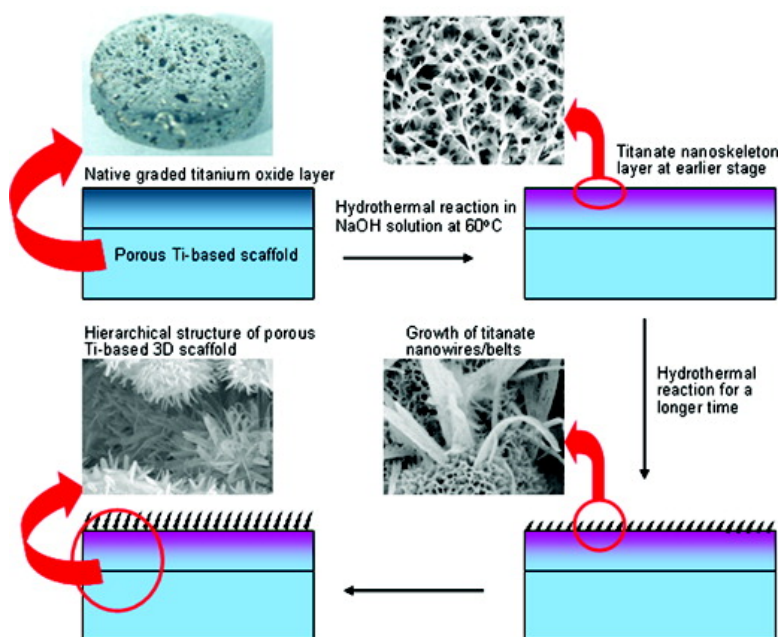Letter

A Biomimetic Hierarchical Scaffold: Natural Growth of Nanotitanates on Three-Dimensional Microporous Ti-Based Metals

Shuilin Wu, Xiangmei Liu, Tao Hu, Paul K. Chu, J. P. Y. Ho, Y. L. Chan, K. W. K. Yeung, C. L. Chu, T. F. Hung, K. F. Huo, C. Y. Chung, W. W. Lu, K. M. C. Cheung, and K. D. K. Luk

More About This Article

Additional resources and features associated with this article are available within the HTML version:

- Supporting Information
- Access to high resolution figures
- Links to articles and content related to this article
- Copyright permission to reproduce figures and/or text from this article

View the Full Text HTML

A Biomimetic Hierarchical Scaffold: Natural Growth of Nanotitanates on Three-Dimensional Microporous Ti-Based Metals

Shuilin Wu,[†] Xiangmei Liu,[†] Tao Hu,[†] Paul K. Chu,*,[†] J. P. Y. Ho,[†] Y. L. Chan,[‡] K. W. K. Yeung,[†] C. L. Chu,[†,§] T. F. Hung,[†] K. F. Huo,[†] C. Y. Chung,[†] W. W. Lu,[‖] K. M. C. Cheung,[‖] and K. D. K. Luk[‖]

Department of Physics & Materials Science, City University of Hong Kong, Tat Chee Avenue, Kowloon, Hong Kong, China, Department of Mechanical Engineering, University of Hong Kong, Pokfulam Road, Hong Kong, China, School of Materials Science and Engineering, Southeast University, Nanjing 210018, China, and Division of Spine Surgery, Department of Orthopaedics and Traumatology, The University of Hong Kong, Pokfulam, Hong Kong, China

ABSTRACT

Nanophase materials are promising alternative implant materials in tissue engineering. Here we report for the first time the large-scale direct growth of nanostructured bioactive titanates on three-dimensional (3D) microporous Ti-based metal (NiTi and Ti) scaffolds via a facile low temperature hydrothermal treatment. The nanostructured titanates show characteristics of 1D nanobelts/nanowires on a nanoskeleton layer. Besides resembling cancelous bone structure on the micro/macroscale, the 1D nanostructured titanate on the exposed surface is similar to the lowest level of hierarchical organization of collagen and hydroxyapatite. The resulting surface displays superhydrophilicity and favors deposition of hydroxyapatite and accelerates cell attachment and proliferation. The remarkable simplicity of this process makes it widely accessible as an enabling technique for applications from engineering materials treatment including energy-absorption materials and pollution-treatment materials to biotechnology.

Tissue failure, particularly that resulting from traumatic or nontraumatic destruction, induces a major health problem that directly affects the quality and length of a patient's life. Today, the need for orthopedic implants is increasing, and more than 500000 bone grafting operations are performed annually in the United States.[1,2] However, traditional tissue repair techniques including tissue grafting and synthetic materials repair exhibit some limitations.[3] For example, although autografting has good clinical applications, its supply is limited, and allografting and xenografting easily induce pathogen transfer or rejection reactions.[4] Moreover, synthetic matrices often integrate poorly with host tissues and result in infection or other adverse body response.[5−7] In view of these restrictions, a number of biocompatible three-dimensional (3D) porous scaffolds have been developed to overcome the traditional limitations and applied to the repair of different tissues.[8−10] Since the surface characteristics of biomaterials such as chemical composition, topography, and roughness are increasingly recognized as crucial factors with regard to tissue acceptance and cell behaviors,[11−13] ideal tissue scaffolds should have hierarchical porous structures. It implies that the scaffolds should have not only macroporous 3D structures on the micro/millimeter scale to facilitate transport of nutrients and tissue ingrowth but also surface features on the nanometer scale. Some recent reports reveal that nanoscale topography of biomaterials significantly influences the adhesion and proliferation of many types of cells such as epithelial cells,[14] osteoblasts,[15] human mesenchymal stem cells (MSCs),[16] phagocyte,[17] as well as protein and genomic response.[18,19] Although there have been scattered reports on the fabrication of both 3D scaffolds on milli/micrometer scales[5,7,20,21] and preparation of nanostructures by layer-by-layer processing,[22] pH-induced self-assembly,[23] electrochemical etching,[24] electron beam lithography (EBL),[16]

* Corresponding author. E-mail: paul.chu@cityu.edu.hk. Phone: 852-27887724. Fax: 852-27887830.
† Department of Physics & Materials Science, City University of Hong Kong.
‡ Department of Mechanical Engineering, University of Hong Kong.
§ School of Materials Science and Engineering, Southeast University.
‖ Division of Spine Surgery, Department of Orthopaedics and Traumatology, The University of Hong Kong.
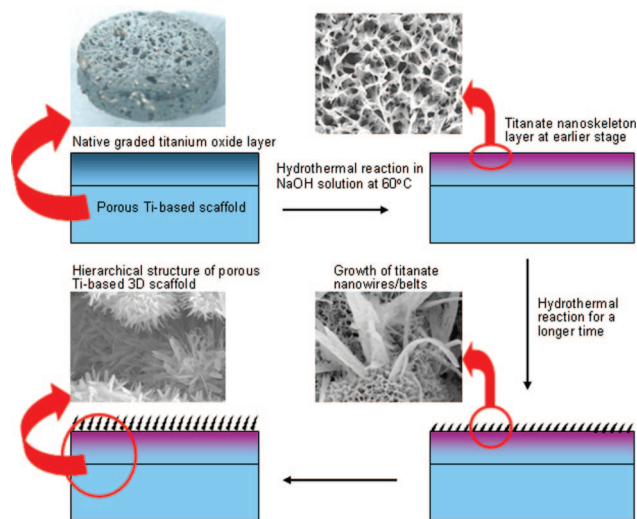
Figure 1. Schematic diagram of the fabrication process of a hierarchical 3D porous Ti-based metal scaffold in 10 M NaOH aqueous solution at a low temperature.

and interference lithography (IL),[25] few studies report the natural growth of bioactive nanophase materials directly on the surface of 3D microporous scaffolds with complex topographies. Herein, we for the first time report the natural growth of bioactive nanotitanate directly on a 3D microporous orthopedic NiTi/Ti scaffold using a facile low-temperature hydrothermal transcription to obtain a hierarchical scaffold similar to the organization structure of human bones.

Ti-based biometals such as Ti, Ti6Al4V, and NiTi are used widely in biomedical fields. As one of the Ti-based metals, the porous NiTi scaffold bodes well for quick repair or substitution of bone or hard tissues due to its unique superelasticity (SE) similar to human bones, good mechanical properties, shape memory effect (SME), controllable 3D porous structures, and excellent cytocompatibility.[26−28] We have produced 3D microporous NiTi and Ti scaffolds using a powder metallurgy (PM) (Supporting Information, Figure S1). Our recent in vivo implant tests in rabbit's tibia for 105 days disclose that bone tissues can grow smoothly into these internal pores and make good contact with the exposed surface of this scaffold (Supporting Information, Figure S2). It is obvious that the reported nanopatterning and assembly techniques are not suitable for the large scale nanopatterning of this scaffold with complex surface topography.[16,22−25] In this work, we achieved a nanostructured surface on the 3D microporous NiTi/Ti scaffold in a concentrated NaOH aqueous solution.

Figure 1 schematically illustrates the fabrication process of this hierarchical 3D porous scaffold. 3D porous Ti-based scaffolds (NiTi/Ti in this work) are immersed in a 10 M NaOH aqueous solution inside a Teflon-lined autoclave. During the heating process, a layer of titanate nanoskeleton forms on the exposed surface in the early stage via the reaction between native titanium oxides and NaOH. As time elapses, some titanate nanobelts and nanowires nucleate and grow on the skeleton, and finally, a hierarchical Ti-based metal scaffold is formed. The big advantage of this hydro-

thermal method is that the alkaline solution can reach the entire exposed surface despite the complex topographies of 3D porous scaffolds due to the non-line-of-sight nature. In contrast, most of the techniques reported heretofore can only be used to fabricate nano/microporous structures on planar materials with simple topographies for tissue engineering.[12,16,17,24] Furthermore, the hierarchical scaffold here has no distinct interface between substrate and nanostructured layer. It is different from hybrid composites filled with a layer of organic nanomatrix by self-assembly,[29] because natural growth directly from the substrate strengthens bonding between the scaffold and nanowires/nanobelts, favoring the formation of a smooth junction between the bone tissue and scaffold and benefiting the long-term fixation of this 3D scaffold. It can possibly extend the lifetime of biomedical implants because materials used today such as titanium, CoCrMo alloy, and so on in bone implants have an average lifetime of only 10−15 years and will not suffice for the aging but active baby-boomer generation.[30] Another outstanding predominance of this hierarchical scaffold is that the inorganic nanostructure layer can significantly improve the surface hydrophilicity whereas the biodegradable polymer scaffolds reported so far including poly(L-lactic acid) (PLLA),[15,31] poly(DL-lactic-co-glycolic acid) (PLGA),[31] poly-styrene (PS),[32] and poly(ethylene terephthalate) (PET),[33] have to undergo surface modification before in vitro or in vivo tests due to their hydrophobic nature.

Figure 2a shows the surface nanostructure of the internal exposed pore of our scaffold after the hydrothermal reaction in sodium hydroxide at 60 °C. A myriad of 1D nanobelts and nanowires form on the wall (Figure 2b) and the bottom (Figure 2c) of the exposed pore. Generally, these 1D nanobelts/nanowires grow directly from the nanoskeleton layer on the surface of the NiTi scaffold perpendicularly (Figure 2d). With respect to the phase compositions and morphologies of the product by the hydrothermal reaction between NaOH aqueous solution and TiO_2 powders or Ti plates, studies in the last decades have shown different results.[34−41] Kasuga et al. proposed that the final hydrothermal product was needle-shaped titania nanotubes after washing with an HCl aqueous solution and distilled water.[42] However, follow-up research confirmed that these products were not titania but rather titanates. Chen et al. synthesized $H_2Ti_3O_7$-type nanotubes,[34] and their work indicated that acidic treatments were not essential. They believed that unstable $Na_2Ti_3O_7$-like nanocrystals formed in the early stage as intermediate phases, and single trititanate layers peeled off from these nanocrystals and curved naturally to form nanotubes. Sun et al. found that pure titanate nanobelts or nanoribbons with a formulation $Na_2Ti_4O_9$ formed from this hydrothermal reaction.[43] More recent works reported the preparation of titanate nanowires,[39,41,44] nanofibers,[35] nanotubes,[36,38,40,45] and nanofilms,[41] with different formulations of $H_2Ti_3O_7 \cdot xH_2O$,[35] $H_xTi_{2−x/4}BOX_{x/4}O_4$ ($x \sim 0.7$),[37] $Na_2Ti_6O_{13}$/ $H_2Ti_3O_7$/ $Na_2Ti_3O_7$,[41,44] $A_2Ti_2O_5 \cdot H_2O$ (A = Na and/or H),[38,45] as well as the general formulation of $Na_yH_{2−y}Ti_nO_{2n+1} \cdot xH_2O$.[39] The common chemistry behind these studies is the ion exchange between Na^+ and H^+ during water or acidic rinsing,
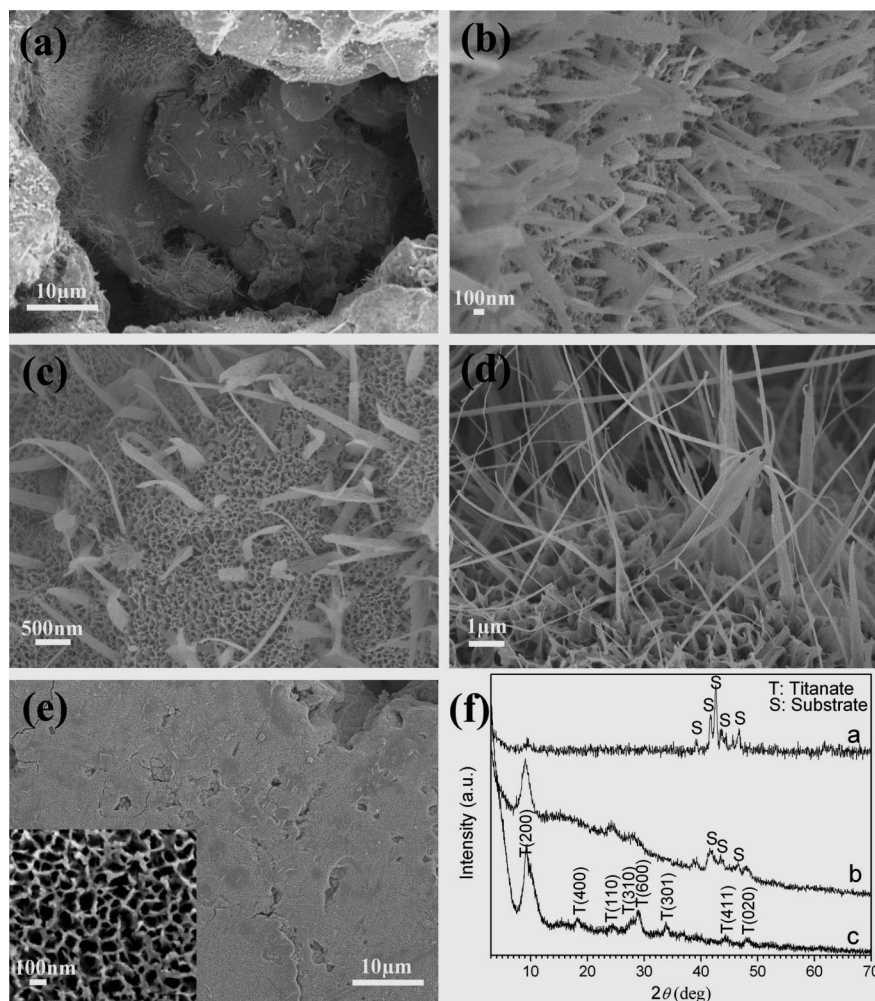
Figure 2. Morphologies of hydrothermally treated 3D porous NiTi scaffold. (a) Typical surface morphology of exposed internal pore after treatment at 60 °C for 240 h. (b) Morphology of the wall of the exposed pore in (a). (c) Morphology of the bottom of the pore in (a). (d) General growth condition of nanowires/nanobelts on the exposed surface after treatment at 60 °C for 240 h. (e) Hydrothermal reaction at 60 °C for 96 h producing a continuous nanoskeleton. (f) XRD patterns for porous NiTi scaffold: trace a, the untreated; trace b, hydrothermal treatment at 60 °C for 240 h; trace c, hydrothermal treatment at 180 °C for 72 h.

resulting in the formation of hydrogen titanate. With regard to the effects of hydrothermal process parameters such as temperature,[41] duration time,[40] NaOH concentration,[41] nature of the acid,[46] and pH value of the acidic wash[38] on the morphology and compositions of produced titanate, there is still controversy. For instance, Riss et al. recently found that $Na_2Ti_3O_7$ nanowires could transform into $H_2Ti_3O_7$ nanotubes only after washing with diluted HCl,[44] while Peng and Chen confirmed that the morphology of nanotitanates was preserved after ion exchange using acidic washing.[41] Armstrong et al.'s experiments indicated that titanate nanotubes formed only at or below 150 °C with a 10 M NaOH and that temperatures over 150 °C induced titanate nanowires.[39] Our results show that both 60 and 180 °C hydrothermal treatments can produce nanobelts and nanowires in a 10 M NaOH solution and the difference is the duration time. The reaction at 60 °C can produce a continuous nanoskeleton for 96 h (Figure 2e), and a longer time (240 h in our work) is necessary to produce the nanowires or nanobelts while 12 and 72 h are sufficient for the occurrence of the nanoskeleton and nanowires at 180 °C, respectively. A possible explanation is that the high temperature provides more energy for

nucleation and growth so that nanotitanates grow faster. It can be confirmed by the thin film X-ray diffraction (XRD) patterns. Trace b (60 °C) in Figure 2f shows the signal from the NiTi(110) substrate after hydrothermal treatment for 240 h, but no signal can be observed from the NiTi in trace c (180 °C for 72 h). The peak positions in traces b and c in Figure 2f can be indexed to $H_2Ti_2O_5 \cdot H_2O$ with an orthorhombic lattice (Joint Committee of Powder Diffraction Standards (JCPDS) card no. 47-124). Since there are no specific ion exchange processes such as long-term deionized water washing or acidic washing in this work, H^+ cannot replace Na^+ massively during the hydrothermal treatment. As shown in the energy-dispersive X-ray spectroscopy (EDS) spectra (insert image of Figure 3), O, Na, and Ti are detected in the scratched 1D nanobelt from the 60 °C treated scaffold (Figure 3). C and Cu arise from the background. Hence, we suggest that the produced nanophase is mainly composed of $Na_2Ti_2O_5 \cdot H_2O$. The Fourier transform infrared spectroscopy (FT-IR) of the surface of the dried specimen shows three absorption bands at 3400, 1630, and 920 cm^{-1} (Supporting Information, Figure S3), indicating the existence of OH bonds in the nanobelts and wires and replacement of some
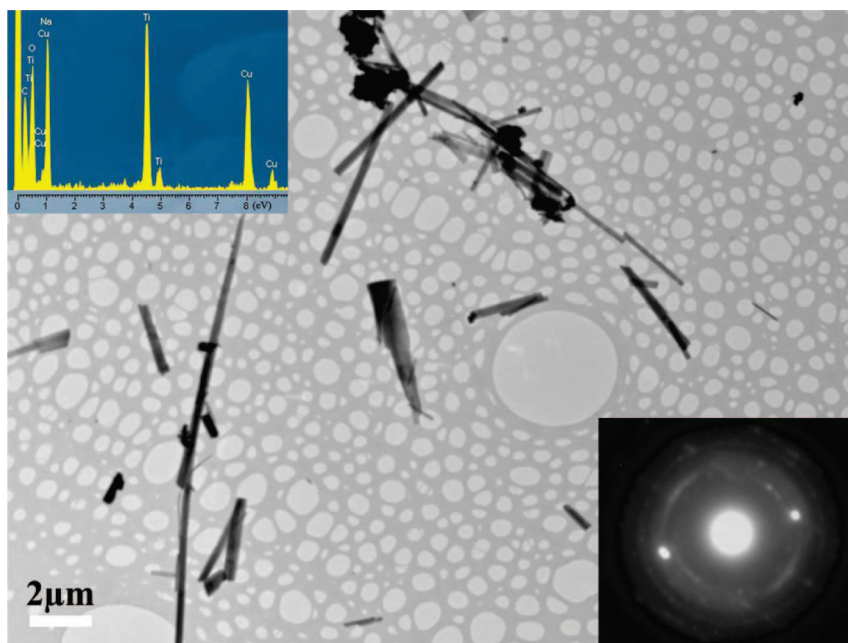
Figure 3. TEM image of scratched nanowires/nanobelts. Top left corner insert EDX pattern shows that elements Ti, Na, and O are detected in the 1D nanobelt. The bottom insert image is the SAED pattern acquired from the nanobelt.
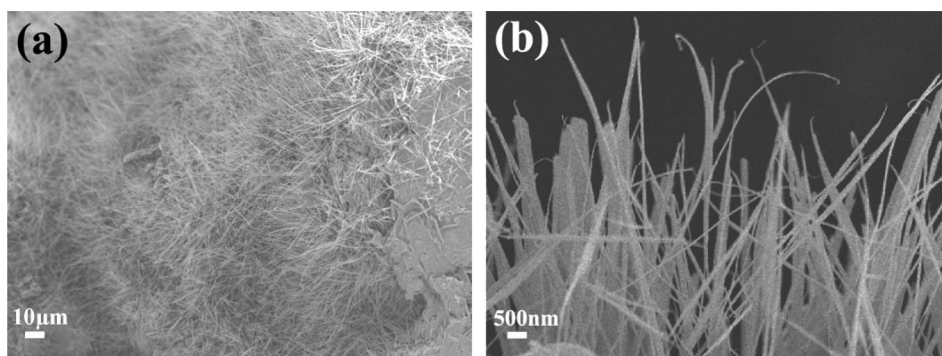

Figure 4. Nanowires and nanobelts on the surface of 3D porous Ti scaffold after hydrothermal treatment at 60 °C for 240 h. (a) General growth condition indicating the large-scale growth of titanates nanowires/belts. (b) Cross-section SEM image of nanobelts and nanowires.

Na^+ cations by H^+.[34,36,45] The selected area electron diffraction (SAED) pattern taken from the big single nanobelt shows that the hydrothermal products are predominantly composed of $Na_2Ti_2O_5 \cdot H_2O$ and traces of other phases (insert image of Figure 3). This layered titanate with crystallized water in the interlayer is unstable under high vacuum.[37] In our work, it is almost impossible to get clearer SAED patterns due to the speedy decomposition or dehydration of the nanobelts under electron impact (Supporting Information, Figure S4). In comparison, the 1D nanobelts prepared from TiO_2 powders in the 10 M NaOH solution by the hydrothermal reaction under the same conditions are stable under high-energy electron beam impact and different SAED patterns have been acquired (Supporting Information, Figure S5). It means that the growth mechanism and structures of the nanotitanates from the porous NiTi scaffold is unlike those from TiO_2 powders in a NaOH solution by the hydrothermal treatment. The latter can fully nucleate and grow randomly on the sites of TiO_2 particles suspended in NaOH solution and have no restrictions, whereas the former can only nucleate on the skeleton with supplies of TiO_2 from the native oxidation and initial oxidation during the PM process. Hence, formation of some nanotitanates is coinstantaneous with the generation of some new titanium oxides during the hydrothermal process. As for the hydrothermal reaction mechanism between Ti and NaOH, Peng and Chen[41] ascribed it to the direct reaction between Ti and NaOH aqueous solution whereas Yang et al.[45] attributed it to the reaction between TiO_2 and NaOH.

As shown in Figure 4a, we can also obtain a large amount of nanowires and nanobelts on the surface of 3D porous titanium scaffold using the same process. An example of the cross section imaged by scanning electron microscopy (SEM) is shown in Figure 4b. Similar to growth on the porous NiTi scaffold, these 1D nanowires and nanobelts grow almost perpendicularly to the substrate and range from about 20 to 1300 nm in width. Our results reveal that other 3D porous Ti-based metals fabricated by PM can be possibly nanostructured by this hydrothermal reaction.
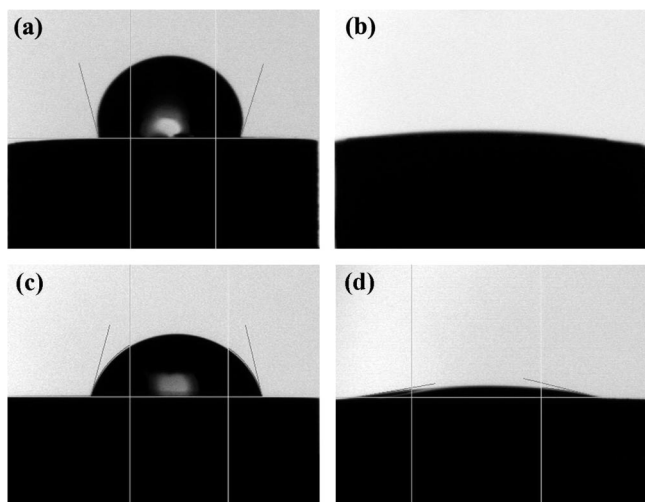
Figure 5. Hydrophilicity of 3D porous Ti-based scaffold. (a) Before hydrothermal treatment of porous NiTi. (b) After hydrothermal treatment of porous NiTi at 60 °C for 240 h. (c) Before hydrothermal treatment of porous Ti. (d) After hydrothermal treatment of porous Ti at 60 °C for 240 h.

It is well-known that wettability is one of the most important properties of biomaterials because cell adhesion and subsequent activities are generally better on hydrophilic surfaces.[47,48] Figure 5 shows the effects of nanotitanates on the hydrophilicity of the porous NiTi/Ti scaffold. The average contact angle is about 106° for water on the untreated porous NiTi scaffold (Figure 5a) whereas the contact angle on the nanotitanate layer is close to zero (Figure 5b). The same phenomenon is observed on the porous Ti scaffold. The mean contact angle is about 81° for water on the untreated porous Ti scaffold (Figure 5c) while the contact angle decreases significantly after nanostructuring by hydrothermal treatment (Figure 5d), indicating that the nanotitanate layer on the porous NiTi scaffold can significantly improve the surface hydrophilicity of the 3D scaffold. The improvement can be attributed to the chemical structure of $Na_2Ti_2O_5 \cdot H_2O$. The hydroxyl and crystallized water in these nanotitanates can easily absorb the water in the environment. In addition, possible Na^+ cation exchange and a large amount of hydroxyl favor deposition of (Ca, P)-containing apatite on the surface of the nanotitanates layer in simulated body fluids (SBF). Another possible factor is that the nanofeatures of titanates such as skeleton, wires, and belts facilitate biomineralization because these nanostructures better resemble the natural characteristics of collagen and hydroxyapatite (HAP), the main constituents of bone. The former consists of arranged arrays of tropocollagen molecules 300 nm long and 1.5 nm wide whereas the plate- or needle-like later is about 40−60 nm long, 20 nm wide, and 1.5−5 nm thick.[2,49] Hartgerink and Woo's results confirm that these nanofibrous materials promote deposition of HAP and proliferation of osteoblasts,[15,23] while earlier research believed that it was bioactive titania or Na^+ cation release from sodium titanate that induced the formation of apatite on Ti-based biomaterials after NaOH treatment.[50,51] Recent research confirmed that a hierarchical nanostructure similar to human bone could influence the conformation of typical adhesive proteins (that

is, fibronectin and vitronectin) present in the media that have been shown to influence osteoblasts behavior.[52] Our preliminary cell culture results also indicate that in comparison with the untreated microporous NiTi sample, the nanostructured titanate surface accelerates cell attachment and proliferation (see Supporting Information, Figure S6).

This study has fully considered the natural hierarchical organization of bone structure and the long-term fixation as well as the hydrophilicity of metal implants for tissue engineering. We have demonstrated the fabrication of a hierarchical 3D microporous NiTi/Ti scaffold via a facile low temperature hydrothermal route. 1D nanotitanates grow naturally on the exposed wall of biocompatible 3D microporous NiTi/Ti scaffold in the form of nanowires and nanobelts on nanoskeletons resembling the lowest hierarchical organization level of human bone. Furthermore, nanotitanates produced in our work have obvious properties that others have never reported, for example, speedy decomposition under high-energy electron impact and superhydrophilicity. The most important point is that the traditional NaOH synthesis route toward titanates is based on TiO_2 powders or Ti plates, but in this work, the raw materials are 3D Ti-based biometals with complex shape. We believe that the remarkable simplicity of this chemical nanostructuring process makes it widely accessible as an enabling technique for applications from engineering materials treatment including energy-absorption materials and pollution-treatment materials to biotechnology.

Supporting Information Available: Details of the fabrication methods and optical image of 3D porous NiTi and Ti by powder metallurgy, hydrothermal transcription process of 3D porous NiTi/Ti scaffold, in vivo testing procedure and histological images of 3D porous NiTi scaffold, FT-IR patterns, TEM image and SAED pattern acquired from TiO_2 powders by the same method as 3D porous NiTi/Ti scaffold, microscopic image of cell growth on microporous NiTi with or without nanotitanate, and in situ TEM images of the speedy decomposition or dehydration of the nanobelts under electron impact in this work. This material is available free of charge via the Internet at http://pubs.acs.org.

References
(1) Parikh, S. N. *Orthopedics* **2002**, *25*, 1301.
(2) Hing, K. A. *Philos. Trans. R. Soc. London, Ser. A* **2004**, *362*, 2821.
(3) Langer, R.; Vacanti, J. P. *Science* **1993**, *260*, 920.
(4) Murugan, R.; Ramakrishna, S. *Tissue Eng.* **2007**, *13*, 1845.
(5) Hollister, S. J. *Nat. Mater.* **2005**, *4*, 518.
(6) Sclafani, A. P.; Thomas, J. R.; Cox, A. J.; Cooper, M. H. *Arch. Otolaryngol. Head Neck Surg.* **1997**, *123*, 328.
(7) Chen, G.; Ushida, T.; Tateishi, T. *Macromol. Biosci.* **2002**, *2*, 67.
(8) Moutos, F. T.; Freed, L. E.; Guilak, F. *Nat. Mater.* **2007**, *6*, 162.
(9) Lin, V. S.; Lee, M. C.; O'Neal, S.; McKean, J.; Sung, K. L. P. *Tissue Eng.* **1999**, *5*, 443.
(10) Drury, J. L.; Mooney, D. J. *Biomaterials* **2003**, *24*, 4337.
(11) Balasundaram, G.; Webster, T. J. *J. Mater. Chem.* **2006**, *16*, 3737.
(12) Lim, J. Y.; Donahue, H. J. *Tissue Eng.* **2007**, *13*, 1879.

(13) Goldberg, M.; Langer, R.; Jia, X. Q. *J. Biomater. Sci., Polym. Ed.* **2007**, *18*, 241.

(14) Andersson, A. S.; Brink, J.; Lidberg, U.; Sutherland, D. S. *IEEE Trans. Nanobiosci.* **2003**, *2*, 49.

(15) Woo, K. M.; Jun, J. H.; Chen, V. J.; Seo, J. Y.; Baek, J. H.; Ryoo, H. M.; Kim, G. S.; Somerman, M. J.; Ma, P. X. *Biomaterials* **2007**, *28*, 335.

(16) Dalby, M. J.; Gadegaard, N.; Tare, R.; Andar, A.; Riehle, M. O.; Herzyk, P.; Wilkinson, C. D. W.; Oreffo, R. O. C. *Nat. Mater.* **2007**, *6*, 997.

(17) Karlsson, M.; Tang, L. *J. Mater. Sci.: Mater. Med.* **2006**, *17*, 1101.

(18) Yap, F. L.; Zhang, Y. *Biosens. Bioelectron.* **2007**, *22*, 775.

(19) Dalby, M. J.; Gadegaard, N.; Herzyk, P.; Agheli, H.; Sutherland, D. S.; Wilkinson, C. D. W. *Biomaterials* **2007**, *28*, 1761.

(20) Jang, J. H.; Dendukuri, D.; Hatton, T. A.; Thomas, E. L.; Doyle, P. S. *Angew. Chem., Int. Ed.* **2007**, *46*, 9027.

(21) Gibson, L. J.; Ashby, M. F. *Cellular Solids: Structure and Properties*; Cambridge Press: Cambridge, 1997.

(22) Jan, E.; Kotov, N. A. *Nano Lett.* **2007**, *7*, 1123.

(23) Hartgerink, J. D.; Beniash, E.; Stupp, S. I. *Science* **2001**, *294*, 1684.

(24) Sun, W.; Puzas, J. E.; Sheu, T. J.; Liu, X.; Fauchet, P. M. *Adv. Mater.* **2007**, *19*, 921.

(25) Jang, J. H.; Ullal, C. K.; Gorishnyy, T.; Tsukruk, V. V.; Thomas, E. L. *Nano Lett.* **2006**, *6*, 740.

(26) Bansiddhi, A.; Sargeant, T. D.; Stupp, S. I.; Dunand, D. C. *Acta Biomater.* **2008**, *4*, 773.

(27) Shabalovskaya, S. A. *Bio-Med. Mater. Eng.* **1996**, *6*, 267.

(28) Wu, S. L.; Chung, C. Y.; Liu, X. M.; Chu, P. K.; Ho, J. P. Y.; Chu, C. L.; Chan, Y. L.; Yeung, K. W. K.; Lu, W. W.; Cheung, K. M. C.; Luk, K. D. K. *Acta Mater.* **2007**, *55*, 3437.

(29) Sargeant, T. D.; Guler, M. O.; Oppenheimer, S. M.; Mata, A.; Satcher, R. L.; Dunand, D. C.; Stupp, S. I. *Biomaterials* **2008**, *29*, 161.

(30) Emery, D. F. G.; Clarke, H. J.; Grover, M. L. *J. Bone Joint Surg.* **1997**, *79*, 240.

(31) Mikos, A. G.; Lyman, M. D.; Freed, L. E.; Langer, R. *Biomaterials* **1994**, *15*, 55.

(32) Neff, J. A.; Caldwell, K. D.; Tresco, P. A. *J. Biomed. Mater. Res.* **1998**, *40*, 511.

(33) Yamamoto, M.; Kato, K.; Ikada, Y. *J. Biomed. Mater. Res.* **1997**, *37*, 29.

(34) Chen, Q.; Zhou, W. Z.; Du, G. H.; Peng, L. M. *Adv. Mater.* **2002**, *14*, 1208.

(35) Zhu, H. Y.; Lan, Y.; Gao, X. P.; Ringer, S. P.; Zheng, Z. F.; Song, D. Y.; Zhao, J. C. *J. Am. Chem. Soc.* **2005**, *127*, 6730.

(36) Kubo, T.; Nakahira, A. *J. Phys. Chem. C* **2008**, *112*, 1658.

(37) Ma, R. Z.; Bando, Y.; Sasaki, T. *Chem. Phys. Lett.* **2003**, *380*, 577.

(38) Tsai, C. C.; Teng, H. S. *Chem. Mater.* **2006**, *18*, 367.

(39) Armstrong, A. R.; Armstrong, G.; Canales, J.; Bruce, P. G. *Angew. Chem., Int. Ed.* **2004**, *43*, 2286.

(40) Elsanousi, A.; Elssfah, E. M.; Zhang, J.; Lin, J.; Song, H. S.; Tang, C. C. *J. Phys. Chem. C* **2007**, *111*, 14353.

(41) Peng, X.; Chen, A. *Adv. Funct. Mater.* **2006**, *16*, 1355.

(42) Kasuga, T.; Hiramatsu, M.; Hoson, A.; Sekino, T.; Niihara, K. *Adv. Mater.* **1999**, *11*, 1307.

(43) Sun, X.; Chen, X.; Li, Y. *Inorg. Chem.* **2002**, *41*, 4996.

(44) Riss, A.; Berger, T.; Stankic, S.; Bernardi, J.; Knzinger, E.; Diwald, O. *Angew. Chem., Int. Ed.* **2008**, *47*, 1496.

(45) Yang, J.; Jin, Z.; Wang, X.; Li, W.; Zhang, J.; Zhang, S.; Guo, X.; Zhang, Z. *Dalton Trans.* **2003**, *20*, 3898.

(46) Bavykin, D. V.; Friedrich, J. M.; Lapkin, A. A.; Walsh, F. C. *Chem. Mater.* **2006**, *18*, 1124.

(47) Liao, H. H.; Andersson, A. S.; Sutherland, D.; Petronis, S.; Kasemo, B.; Thomsen, P. *Biomaterials* **2003**, *24*, 649.

(48) Liu, X. H.; Ma, P. X. *Ann. Biomed. Eng.* **2004**, *32*, 477.

(49) Suchanek, W.; Yoshimura, M. *J. Mater. Res.* **1998**, *13*, 94.

(50) Wen, H. B.; de Wijn, J. R.; Cui, F. Z.; de Groot, K. *J. Biomed. Mater. Res.* **1998**, *41*, 227.

(51) Kim, H. M.; Miyaji, F.; Kokubo, T.; Nishiguchi, S.; Nakamura, T. *J. Biomed. Mater. Res.* **1999**, *45*, 100.

(52) Stevens, M. M.; George, J. H. *Science* **2005**, *310*, 1135.

NL802145N